Title

Multiphase chemistry in the troposphere: It all starts … and ends … with gases

Journal

International Journal of Chemical Kinetics, 51(10)

ISSN

0538-8066

Author

Finlayson-Pitts, Barbara J

Publication Date

2019-10-01

DOI

10.1002/kin.21305

Received: 26 March 2019 | Revised: 8 May 2019 | Accepted: 8 May 2019

DOI: 10.1002/kin.21305

WILEY

ARTICLE

Multiphase chemistry in the troposphere: It all starts … and ends … with gases

Barbara J. Finlayson-Pitts

Department of Chemistry, University of California, Irvine, Irvine, California

Correspondence
Barbara J. Finlayson-Pitts, Department of Chemistry, University of California, Irvine, Irvine, CA 92697-2025.
Email: bjfinlay@uci.edu

Funding information
Army Research Office, Grant/Award Number: W911NF1710105; National Science Foundation, Grant/Award Numbers: # 1647386, #1707883

Abstract

When the phenomena of smog and acid deposition were first recognized, it was largely gas phase chemists and photochemists who leapt into the fray to untangle the sources and chemistry involved. Over time, the importance of multiphase chemistry was recognized, as illustrated in a dramatic manner with the discovery of the Antarctic ozone hole which is driven by heterogeneous chemistry on polar stratospheric clouds. Since then, it has become clear that multiphase chemistry is central to both the lower and upper atmosphere and that this deeply intertwines interactions between the gas and condensed phases in the atmosphere. As a result, it can be argued that multiphase atmospheric chemistry begins … and ends… with gases. This paper is based on the 2018 Polanyi Medal award presentation at the 25th International Symposium on Gas Kinetics & Related Phenomena and traces research carried out in the author's laboratory on multiphase chemistry over a number of decades. While a great deal has been learned about these processes, they remain one of the areas of greatest uncertainty in understanding atmospheric composition, air quality, chemistry, and climate change.

KEYWORDS

atmosphere, gas, kinetics, multiphase, particles

1 | INTRODUCTION

I am delighted and honored to be awarded the 2018 Polanyi Medal of the Royal Society of Chemistry. Given the previous awardees, it is in august company indeed to find oneself. This paper is based on the award talk given at the 25th International Symposium on Gas Kinetics & Related Phenomena held in Lille in July 2018. The theme of that talk was my history in the field of gas phase and multiphase kinetics relevant to atmospheric chemistry over more than four decades, and as a result, it is very BJFP-lab centered. I apologize in advance to many colleagues whose work is not cited in the interests of following the award presentation and for brevity.

I have watched the field of atmospheric chemistry evolve from its birth in the gas phase chemistry and photochemistry community to the point that delineation of gases, clusters, and particles is no longer always obvious. Multiphase interactions between gases, liquids, and solids are ubiquitous in the atmosphere and ultimately, one can argue, both start and end with gases.

My interest in atmospheric chemistry began in an undergraduate physical chemistry laboratory where my faculty mentor, Professor Ray March, talked about the chemistry of the aurora. It was my first introduction to the idea that the atmosphere was really a giant, complex, constantly changing chemical reactor. At that time (1969), the field of atmospheric chemistry per se did not exist, but scientists in physical, organic, and analytical chemistry had been drawn into understanding the phenomenon of smog formation which was clearly damaging human health, visibility, plants, and materials. The seminal work in the 1950s of Professor Arie Haagen-Smit, an organic chemist at Cal Tech, had established that gas phase organic compounds and oxides of nitrogen, when irradiated, form ozone, particles, and other manifestations of smog. While NO_2 photolysis was established to be the source of anthropogenic ozone, the reactions responsible for

converting NO (the major oxide of nitrogen emission from fossil fuel combustion) to NO_2 and the role of the organics remained obscure. Indeed, it was not until about 1970 that the OH free radical was established as a major oxidant[1–4] that converted organics to alkylperoxy radicals that then oxidized NO to NO_2. However, relatively little was known about the fundamental kinetics and mechanisms involved not only in OH reactions with organics but also the subsequent free-radical induced chemistry.

The most obvious manifestation of smog formation was light scattering by particles which caused significant loss of visibility. However, it has become clear over the years that particles do not just represent an aesthetics problem associated with visibility reduction[5] but also have severe health impacts.[6,7] These include impacts[8] on the heart, lungs, reproductive system, and, more recently, particles have been associated with neurodegenerative diseases such as dementia[9–11] as well as cognitive performance.[11] Particles also play a major role in climate[12–14] both directly by scattering incoming solar radiation and indirectly by acting as seeds for cloud formation.[15] These direct and indirect effects cause a decrease in radiative forcing (cooling). While light absorbing particles such as soot and organic particles containing "brown carbon" contribute to positive radiative forcing (warming), the overall impact of particles is a net decrease in radiative forcing that in part counteracts the warming due to greenhouse gases.[16]

Some particles are directly emitted (eg windblown dust, soot from diesel engines, fly ash from coal-burning power plants), but a major source of airborne particles is gas phase reactions to form highly oxidized, low volatility products that either nucleate to form new particles or add to existing particles to grow them.[17,18] Predicting particle concentrations and size distributions from such sources requires a detailed understanding of gas phase kinetics and precursor oxidation mechanisms, as well as how gases interact with particles. Such new particle formation and growth processes involve gases, clusters, and, finally, liquid or solid particles, supporting all three as the basis for understanding and quantifying multiphase atmospheric processes. Gases also react with condensed phases in the atmosphere, and reactions on and inside particles can provide new products that undergo further chemistry.[19] Finally, chemistry and photochemistry within particles can result in the formation of more volatile species which are emitted into the gas phase, contributing to the budgets of those trace gases.[20,21] So in short, it all starts … and ends … with gases.

Four examples of multiphase reactions in the lower atmosphere (troposphere) are described below. The first involves the formation of new particles from the reactions of methanesulfonic acid, $CH_3S(O)(O)OH$, (MSA) with amines in the gas phase. The second example describes some studies designed to probe the molecular interactions of incoming gases with the surfaces of proxies for organic particles in air to understand uptake and growth mechanisms of these particles. The third example involves reactions of gases with sea salt particles, and, the fourth, the photochemistry of neonicotinoid pesticides that undergo unusual chemistry to release unexpected gas phase products. It is hoped that these four examples illustrate the seminal role of gas phase kinetics and mechanisms in understanding our complex atmosphere with sufficient confidence to be able to make predictions that can be used in the development of optimal control strategies to address human health, climate, and visibility.

2 | NEW PARTICLE FORMATION FROM THE REACTIONS OF METHANESULFONIC ACID WITH AMINES

The combustion of sulfur-containing fossil fuels emits SO_2, which is oxidized in air to sulfuric acid, H_2SO_4 (SA).[22,23] Gas phase SA reacts efficiently with the atmospheric bases ammonia and amines,[24–28] which are ubiquitous in air,[29,30] generating low volatility clusters which can form and/or grow particles. Once they reach ~100 nm diameter, particles can act as cloud condensation and ice nuclei,[15,31] scatter light efficiently,[5] and reach the deep, alveolar region of the lung where gas exchange occurs.[32] However, there are other sources of sulfur-based particles, for example, organosulfur compounds such as dimethyl sulfide, CH_3SCH_3 (DMS), emitted by biological processes in coastal areas, and their oxidation products.[33,34] Products of the oxidation[35,36] include not only SO_2 and hence ultimately sulfuric acid but also another strong acid, MSA. While a great deal is known about the kinetics and mechanisms of the steps involved in converting CH_3SCH_3 into MSA,[35,36] there are some key missing steps that are ripe for investigation. For example, the $CH_3S(O)(O)O$ radical can be formed by various pathways but those leading from the radical to MSA are not clear. Hydrogen abstraction from organics has been proposed, but to the best of the author's knowledge there are no experimental studies of these reactions. Theoretical studies suggest hydrogen abstraction from formaldehyde has a submerged barrier and should be very fast (Figure 1).[37] While the reaction with CH_4 has a positive barrier (Figure 1) and is expected to be slow, reactions with larger organics, particularly those with weaker C−H bonds such as allylic C-H may be much faster than CH_4, and may also contribute to the conversion of $CH_3S(O)(O)O$ to MSA.

Although MSA does not form particles as efficiently with water under atmospheric conditions as sulfuric acid does,[38–40] we demonstrated that it can form a large number of new particles in the presence of ammonia and/or amines.[41] MSA with ammonia is least efficient in forming particles, whereas methylamine (MA) is the most efficient and di- and trimethyl

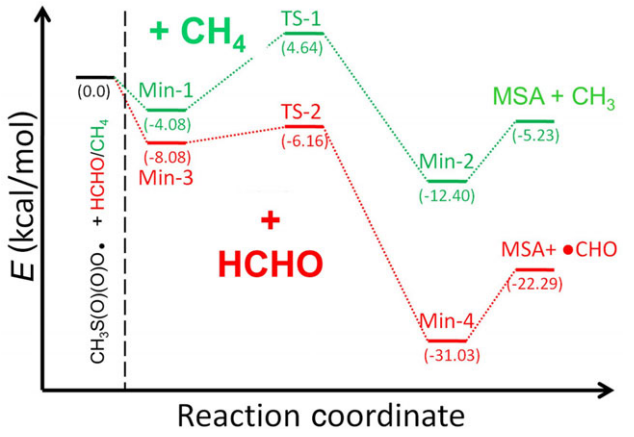

FIGURE 1 Predicted energies in the reactions of the $CH_3S(O)(O)O$ radical with HCHO and CH_4 [Ref. 37] [Color figure can be viewed at wileyonlinelibrary.com]

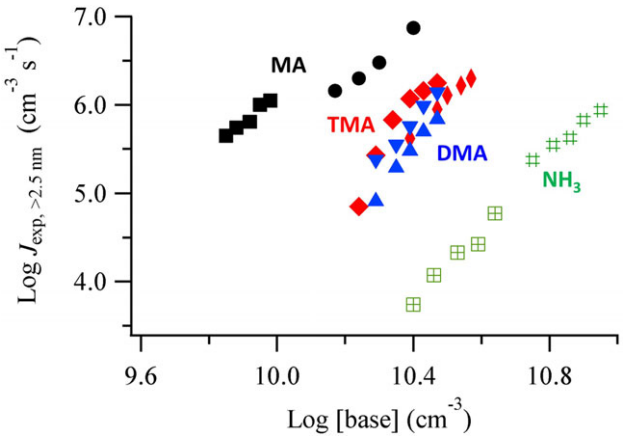

FIGURE 2 Rates of formation of detectable (2.5 nm) particles ($J_{exp2.5\ nm}$) from 4×10^{10} cm^{-3} MSA reacting with ammonia and amines (MA = methylamine; DMA = dimethylamine and TMA = trimethylamine) at 55% RH as a function of base concentration[42] [Color figure can be viewed at wileyonlinelibrary.com]

amine (DMA and TMA, respectively) are intermediate in this regard (Figure 2).[42] Interestingly, if water vapor is introduced with the other reactants (as opposed to dry particles exposed to water vapor after formation), it significantly enhances new particle formation (Figure 3).[41–45] Theoretical studies have been carried out to elucidate the reasons that water plays such an important role.[37,41–48] As an example, Figure 4 shows the calculated lowest energy structures of two small MSA-TMA-water clusters that are stable.[41] Water provides additional hydrogen bonding sites to which incoming gas molecules can bind, growing the particles to detectable sizes, in this case ~2.5 nm. Particles of this size are much larger than the clusters shown in Figure 4, so that experimentally it is the combination of new particle formation and growth to this size that operationally defines particle formation in this system. In contrast, quantum chemical calculations suggest that water added to larger clusters formed from MSA-MA resides on the surface or for increasing numbers of waters, inside the clusters.[46,48]

An important question is how important MSA is for particle formation in air compared to sulfuric acid. A classic case is the South Coast Air Basin in Southern California where the ports are a major source of anthropogenic SO_2 and organosulfur compounds such as DMS are produced by biological processes in the ocean. Specific unknowns are as follows: (1) To what extent does MSA contribute to particle formation under current conditions in a coastal urban area? (2) If anthropogenic SO_2 is eliminated in the future with phaseout of fossil fuel combustion, what will the contribution of MSA be to airborne particles? To answer these questions, modeling of this region was undertaken[37] using the University of California, Irvine-California Institute of Technology (UCI-CIT) regional airshed model[49] that included SO_2 emissions from the ports and some other, smaller, sources as well as DMS emissions from the coastal regions.[37] Figure 5 is a schematic of the model and the domain covered by the model. It divides the region into 80 cells in the E-W direction, 30 cells N-S, and 5 cells vertically. Emissions, meteorology, and chemistry are integrated to predict the concentrations of various species as a function of time and location. In that study, gas phase concentrations of SA and MSA were calculated for the period 2011-2013 as proxies for particle formation from these two precursors, since their major sink in each case will be particle formation and growth. Concentrations at noon are shown in Figure 6A for SA and 6C for MSA. The anthropogenic emissions of SO_2 were then assumed to be zero, and the MSA and SA concentrations due only to the remaining biological emissions were calculated. Note that MSA concentrations do not change significantly under this scenario since they only have a biogenic origin. Figure 6B shows the new SA concentrations with anthropogenic SO_2 emissions removed. Because SO_2 and hence SA is also generated from organosulfur oxidation, small amounts of sulfuric acid remain when the anthropogenic sources fall to zero. However, peak concentrations of SA drop by two orders of magnitude, and MSA and SA are now more comparable in concentration and hence in their potential contribution to airborne particles. Given that the net effect of such particles on climate is cooling, such a decrease in particle formation will provide less counterbalance to the warming due to greenhouse gases, leading to even faster climate change than is currently the case. On the other hand, a key point is that the decreased particle concentrations will lead to less deleterious impacts on human health as well as improved visibility.[7,16,50]

3 | MOLECULAR BASIS OF SECONDARY ORGANIC AEROSOL PARTICLE GROWTH

Organic compounds comprise a large fraction of airborne particles[51,52] and have many sources, both anthropogenic and

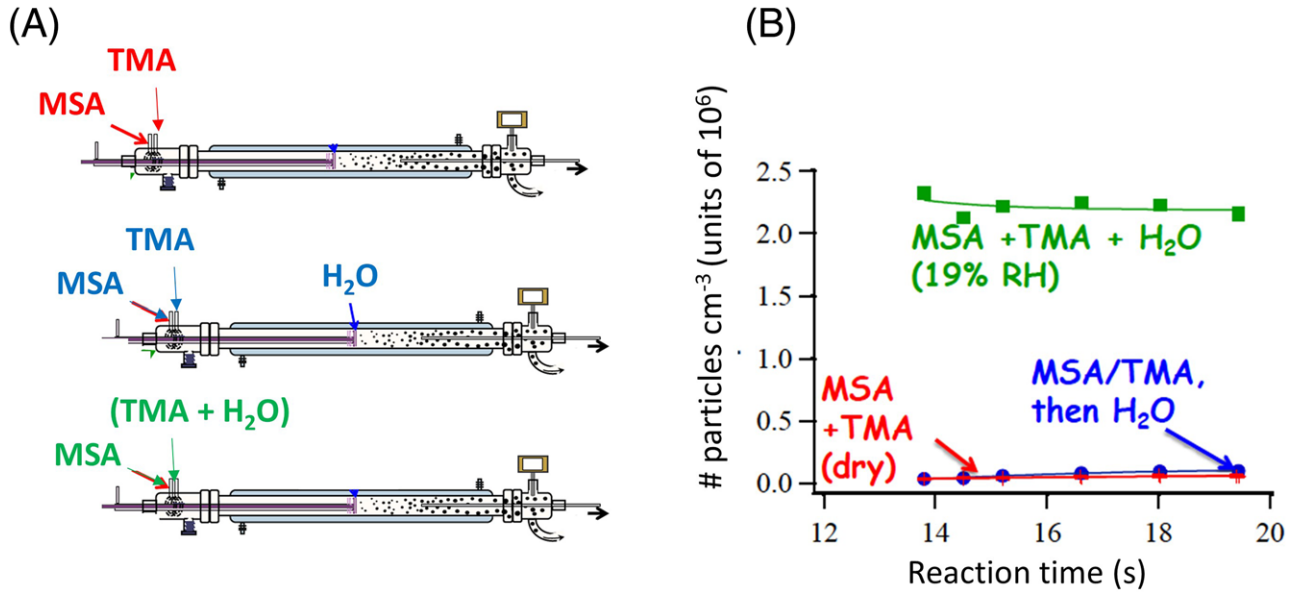

FIGURE 3 (A) Flow tube configurations used for studying particle formation from MSA reactions with amines in the absence and presence of water vapor; (B) particle formation from MSA and trimethylamine (TMA) as a function of reaction time under dry conditions (red), under dry conditions with water added later at the downstream spokes (blue), and at 19% RH where all three are present simultaneously, with water added through the upstream spokes (green)[44] [Color figure can be viewed at wileyonlinelibrary.com]

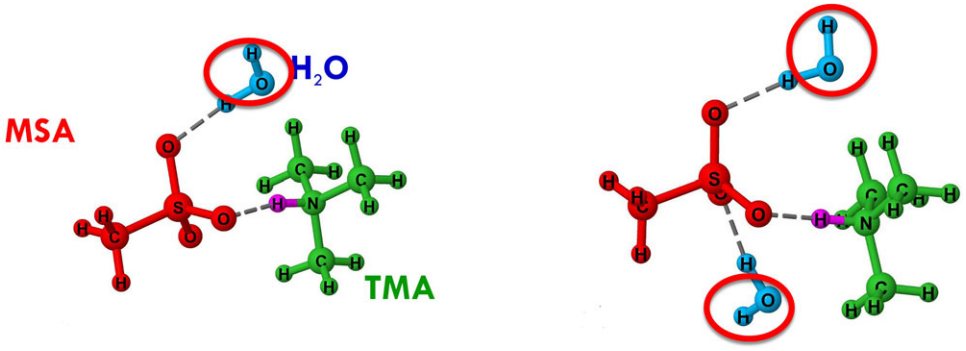

FIGURE 4 Theoretically predicted structures of some clusters of trimethylamine and MSA with one or two water molecules[41] [Color figure can be viewed at wileyonlinelibrary.com]

biogenic. Figure 7 shows typical contributions of organics (green), sulfate (red), nitrate (blue), ammonium (yellow), and chloride (purple) to the portions of particles that volatilize at 600°C,[51] illustrating that organics are a significant component at all locations.

Organic particles that are formed in air from gas phase reactions are known as secondary organic aerosol (SOA). We prefer to designate these as SOA particles, since "aerosol" is formally defined as the combination of particles and the gas in which they are entrained.[5] It has been historically assumed in models that these organic particles are liquid, so that diffusion and exchange with the gas phase is fast. In this case, solubility and volatility are expected to play a major role in determining uptake from the gas phase that will control particle growth. However, about 10 years ago, it was reported that SOA particles can bounce off the surfaces of impactors used to collect them in a manner that suggested they were not lower viscosity liquids, but rather higher viscosity, semisolids.[53,54] This has since been confirmed by a number of groups.[55–63] For example, Figure 8A shows a custom-designed impactor used to collect particles on an attenuated total reflectance infrared-transmitting crystal.[60] The impaction patterns of deliquesced Na_2SO_4 particles (Figure 8B) can be compared to those from α-pinene ozonolysis (Figure 8C).[60] The deliquesced particles impact immediately below the orifice holes along the impactor centerline, forming a corresponding line of collected particles. The SOA particles, however, form a "cloud" located toward the edge of the crystal, indicating they have bounced from the point of initial impact and hence must be a relatively high viscosity material, likely a mixture of higher molecular mass organics. Interestingly, there was a hint of the presence of such compounds

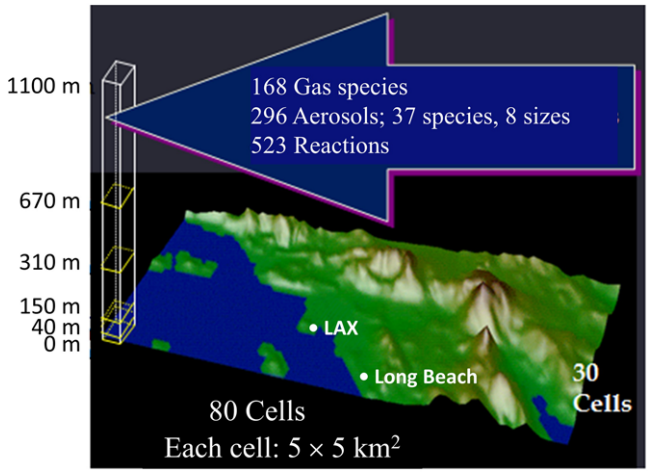

FIGURE 5 Schematic of the UCI-CIT airshed model of Southern California[49] [Color figure can be viewed at wileyonlinelibrary.com]

in particles many decades ago from electron microscopy images of haze particles collected in the Los Angeles area (Figure 9).[64] These images were interpreted as arising from particles that were coated with a nonvolatile organic material. Under the vacuum conditions used to obtain the images, water and other high volatility components evaporated from the particles, leaving the organic material in a shrunken and wrinkled form.

Typical timescales for diffusion in particles as a function of viscosity/diffusion coefficients are shown in Figure 10.[65] For a 100 nm particle, they range from milliseconds for liquid particles to years for semisolid particles. This dramatically impacts exchange with the gas phase and how the particles incorporate gases into their bulk to grow to larger sizes. Figure 11 is a schematic that illustrates this difference. The predictions of modeling studies of particle growth in the

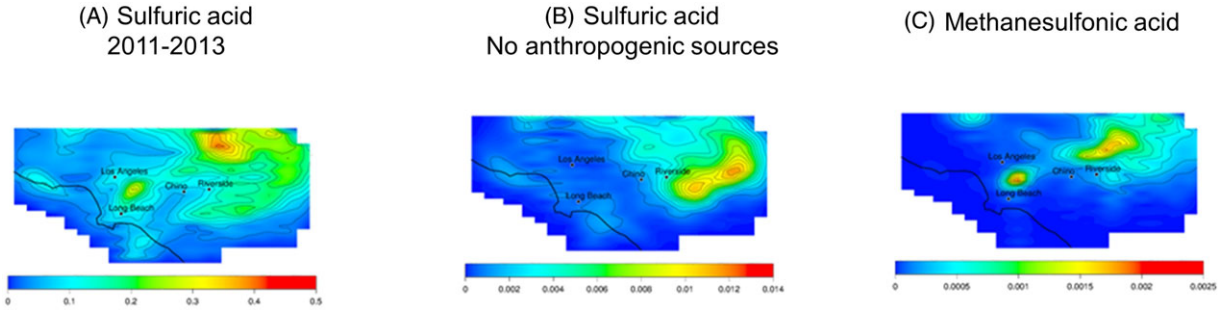

FIGURE 6 Model-predicted gas phase concentrations (ppb) of sulfuric acid (SA) and MSA at noon under three scenarios: (A) SA representative of the years 2011-2013, (B) SA with fossil fuel emissions removed, and (C) MSA (results the same for with and without anthropogenic emissions since MSA sources are biogenic)[37] [Color figure can be viewed at wileyonlinelibrary.com]

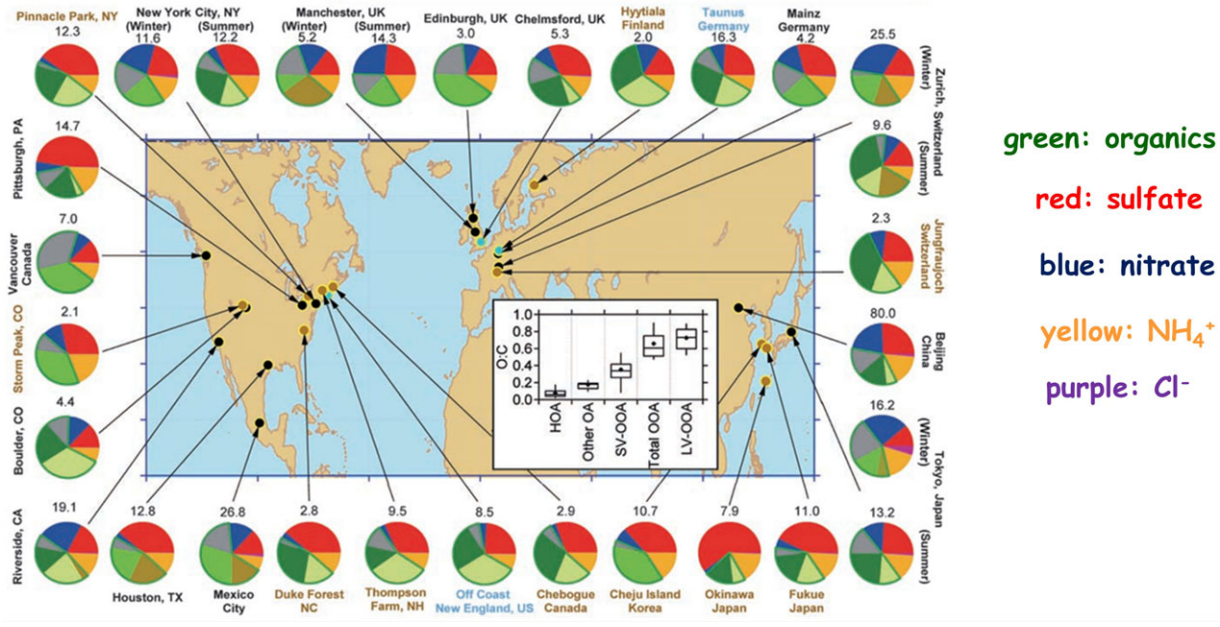

FIGURE 7 Aerosol mass spectrometry measurements of the nonrefractory components of airborne particles at various locations around the world[50] [Color figure can be viewed at wileyonlinelibrary.com]

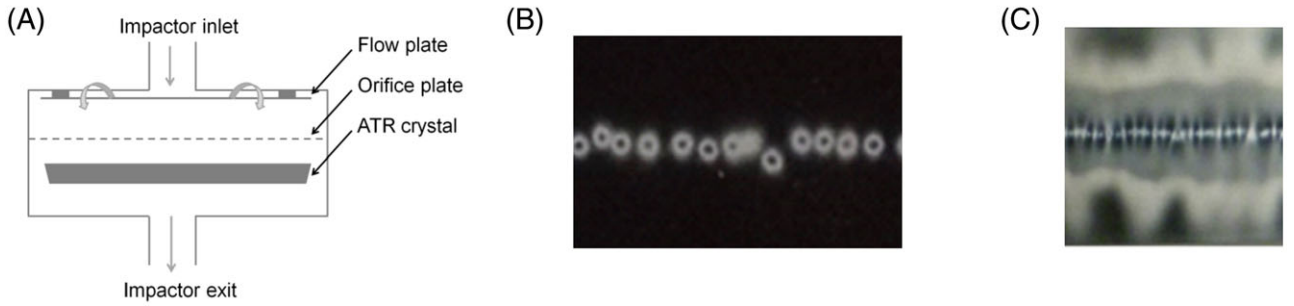

FIGURE 8 (A) Schematic of impactor, (B) impaction patterns for deliquesced Na_2SO_4 particles showing the particles are collected where they impact directly under the holes of the orifice plate, and (C) impaction patterns for SOA particles from α-pinene ozonolysis showing particle bounce from the initial points of impaction[59] [Color figure can be viewed at wileyonlinelibrary.com]

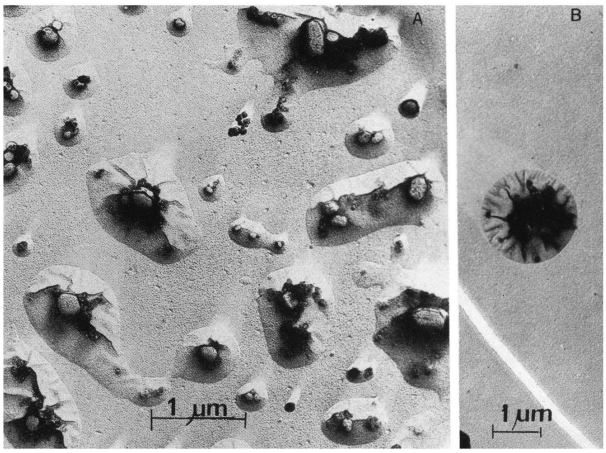

FIGURE 9 Electron microscopy images of haze particles collected from air in Los Angeles[63]

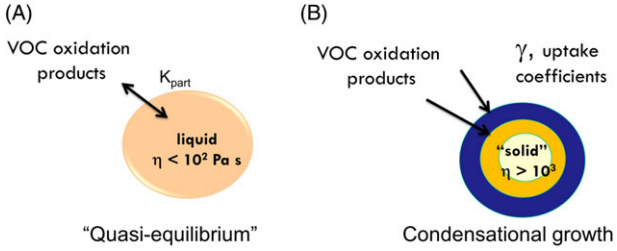

FIGURE 11 Schematic of uptake of VOC oxidation products into SOA particles under two scenarios: (A) low viscosity ($\eta < 10^2$ Pa s), liquid particles where diffusion in the particles is rapid and the partitioning coefficient K_{part} is determining and (B) higher viscosity ($\eta > 10^3$ Pa s) solid particles where uptake occurs via condensation on the surface and the uptake coefficient γ is determining [Color figure can be viewed at wileyonlinelibrary.com]

atmosphere are, not surprisingly, quite different for the two assumptions.[66]

For semisolids, the probability of incorporation of a gas molecule impacting on the surface of an SOA particle into the bulk of the particle to cause growth will be determined by a number of factors. A major one is the nature and strength of the intermolecular forces between the gas molecule and the surface functional groups. The solubility of the gas in the bulk of the particle will also depend on the intermolecular forces, but those in the bulk may differ from those with the surface if the functional group distribution on the surface differs

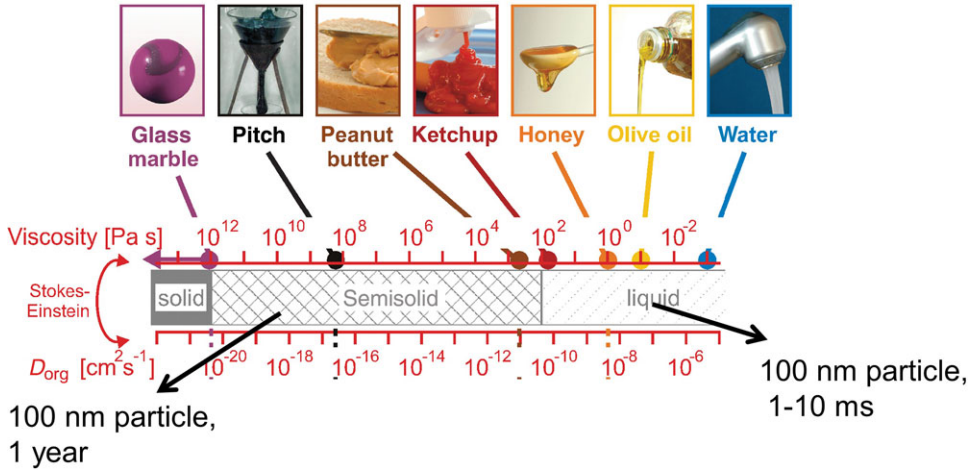

FIGURE 10 Viscosity and diffusion coefficients for some common materials and diffusion times for 100 nm particles of low and high viscosity[64] [Color figure can be viewed at wileyonlinelibrary.com]

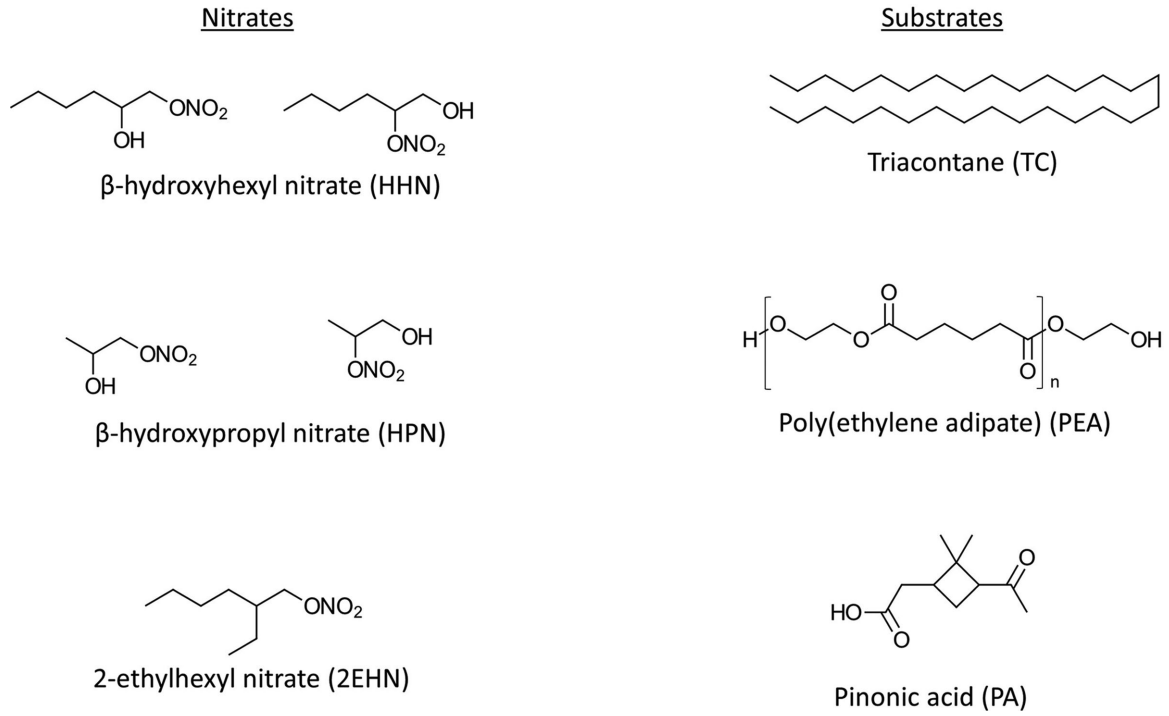

FIGURE 12 Structures of the organic thin film substrates TC, PEA, PA, and the gaseous organic nitrates β-hydroxyhexyl nitrate (HHN), β-hydroxypropyl nitrate (HPN), and 2-ethylhexyl nitrate (2EHN) whose uptake into the films was measured[68]

from the bulk. Some evidence for such a difference has been reported; for example, in aggregates formed from the ozonolysis of alkene self-assembled monolayers[67] and in SOA particles from α-pinene ozonolysis,[68] the O:C ratio was reported to be lower on the surface than found in the bulk. Such a difference between the intermolecular interactions at the surface and the bulk would be manifested in different trends for uptake coefficients (surface property) compared to solubility (bulk property).

To probe for potential differences in the trends of uptake coefficients versus solubility, the incorporation of a series of organonitrates into thin films was measured.[69] These thin films were solid organics of known composition containing functional groups that are commonly found in SOA particles, as well as SOA particles from α-pinene ozonolysis. The selected substrates and the gases are shown in Figure 12. Two of the gases, 2-ethylhexylnitrate (2EHN) and hydroxypropylnitrate (HPN), have similar vapor pressures (18 and 16 Pa, respectively) but different functional groups and therefore different intermolecular interactions with substrates. Thus the longer alkyl chain in 2EHN results in stronger dispersion forces compared to HPN, but HPN has the possibility of hydrogen bonding via the −OH group. On the other hand, while HPN and hydroxyhexylnitrate (HHN) both have −OH and $-ONO_2$ groups, HHN has a much lower vapor pressure (0.85 Pa) because of the long alkyl chain. The substrates range from the nonpolar triacontane (TC) to the polar poly(ethylene adipate) (PEA) to polar with strong hydrogen-bonding possibilities, pinonic acid (PA).

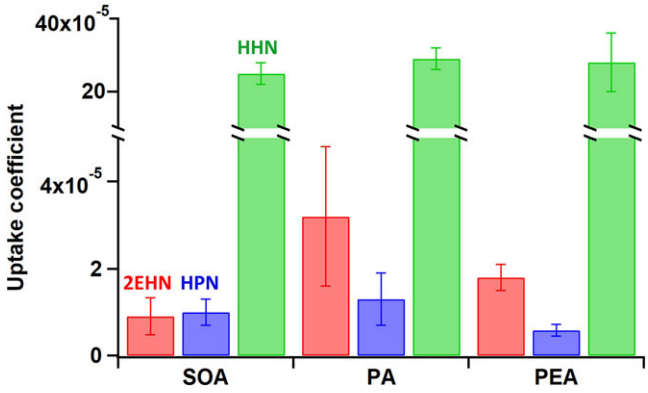

FIGURE 13 Uptake coefficients for 2EHN, HPN, and HHN on SOA, PA, and PEA, respectively[68] [Color figure can be viewed at wileyonlinelibrary.com]

Figure 13 shows the uptake coefficients on SOA particles from α-pinene ozonolysis, PA, and PEA. The uptake coefficients for 2EHN on PEA and PA are greater than those for HPN, which was initially surprising, given the −OH group in HPN and polar groups in PEA and PA. Quantum chemical calculations on the organonitrates interacting with PEA provided some insight. As seen in Figure 14A, the most stable configuration for 2EHN is one that aligns the alkyl chain with the surface, which is not very sterically demanding. The major interaction with HPN is a hydrogen bond to a C=O at the surface (Figure 14B), so that if the initial point of contact of HPN with PEA is not with the C=O but rather with the

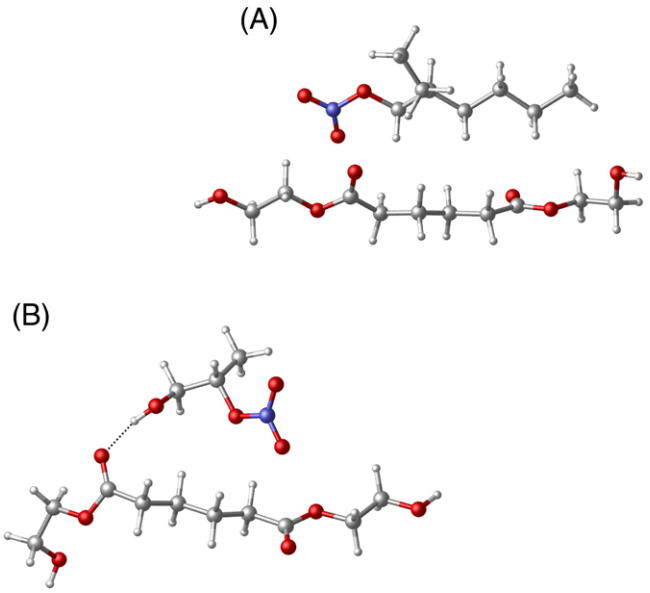

FIGURE 14 Optimized structures for (A) one 2EHN molecule binding to one PEA subunit, and (B) one HPN molecule binding to one PEA subunit[68] [Color figure can be viewed at wileyonlinelibrary.com]

alkyl portion of the molecule, it will not be captured. Thus even though the binding energy of 2EHN (11.8 kcal mol^{-1}) is less than that of HPN (13.5 kcal mol^{-1}), its initial uptake is higher. Interestingly, the uptake coefficient for 2EHN on collected SOA particles is smaller than on PA or PEA. It is likely that the surface of SOA is highly oxidized and does not contain significant regions of nonpolar moieties to which 2EHN can readily bind through dispersion forces as is the case for PA and PEA.

Figure 15 shows the partition coefficients measured for dissolution of the gases into the films at equilibrium. HPN is more soluble than 2EHN in SOA particles (Figure 15 inset). This is not surprising since HPN is more polar and hence interact more strongly with the polar products present in SOA particles. The fact that there is a difference in solubility but not in uptake coefficients highlights the issue that initial interactions with the surface are not necessarily well predicted by bulk solubility. For example, HHN uptake is similar across substrates, while its solubility is quite different, illustrating the importance of understanding the nature of the surfaces of organic particles.

There are very few techniques that differentiate the particle surface composition from that of the bulk, although as discussed earlier, there are some data suggesting they are different.[67,68] Some progress has been made in this regard using new, ambient ionization techniques.[70] In addition to the lack of sample preparation required, these methods can provide molecular level information. For example, extractive electrospray ionization[71] and easy ambient sonic spray ionization (EASI)[72] have both been shown to be capable of sampling mainly the surfaces of organic particles suspended in air without collection or other sample handling. In a recent study from this lab,[72] glutaric acid (GA) core particles were coated with increasing thicknesses of malonic acid (MA), and sampled using EASI-MS. Figure 16A shows the increase in the signal from the MA coating and decrease in that from the GA core as the coating thickness (as indicated by the temperature used to volatilize the MA to coat the GA particles) increased. Figure 16B shows the corresponding increase in the ratio of coating (MA) to core (GA) as a function of the coating temperature/coating thickness, supporting preferential detection of the surface. Also shown is the ratio averaged over the entire particle (bulk analysis from particles collected on a filter and extracted), which is much smaller since it measures the coating and the entire core. These are promising techniques for molecular level detection of the surface of organic particles,

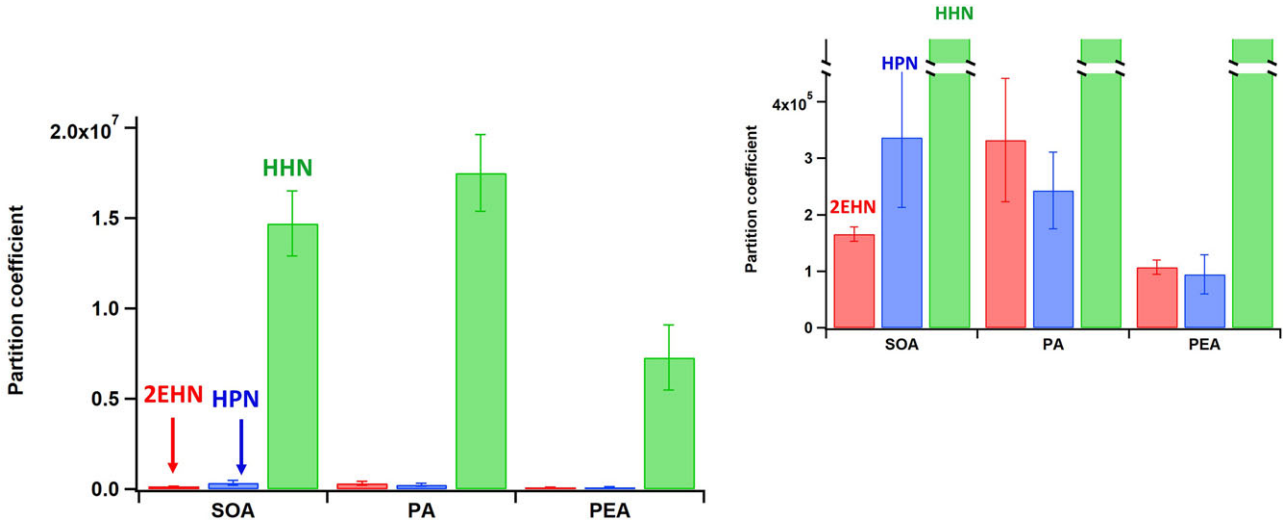

FIGURE 15 Partition coefficients for the organic nitrates 2EHN, HPN, and HHN into SOA, PA, and PEA.[68] The inset is an expanded view to show 2EHN and HPN [Color figure can be viewed at wileyonlinelibrary.com]

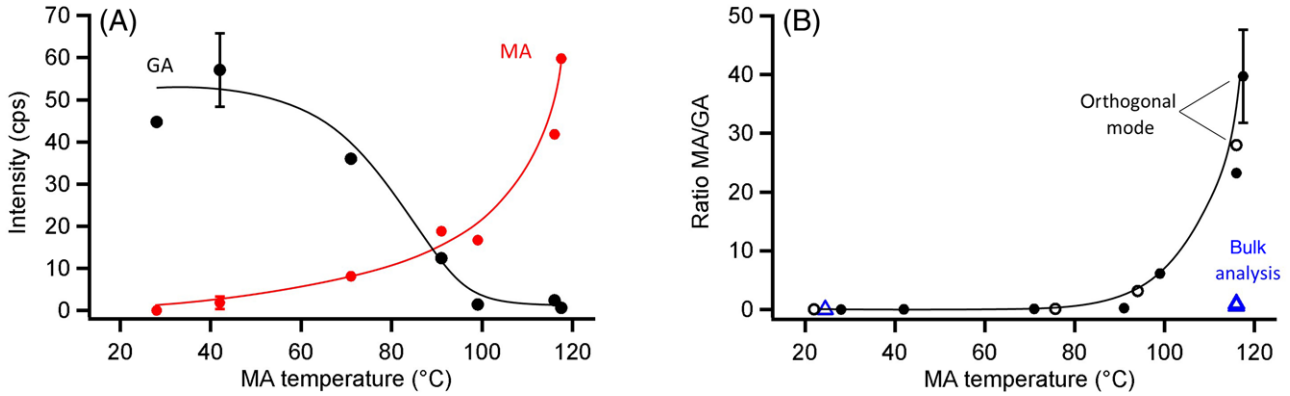

FIGURE 16 (A) Signal intensities of 220 nm GA particles (black) coated with MA (red) as a function of MA coating reservoir temperature (MA coating thickness); (B) black circles are MA/GA ratio calculated from EASI-MS data in (A). Blue triangles are the bulk analysis of filter collected and extracted MA-coated 220 nm GA particles. The black filled and black open circles are data from replicate experiments[71] [Color figure can be viewed at wileyonlinelibrary.com]

which is needed for predicting particle growth by uptake from the gas phase.

In short, understanding and quantifying the factors that control the growth of organic particles via uptake from the gas phase onto/into particles is still in its infancy, but is a critical area for predicting visibility, climate change and health effects.

4 | REACTIONS OF GASES WITH PARTICLES AS A MEANS OF ALTERING THE OXIDANT CAPACITY OF THE ATMOSPHERE

Wave action generates sea salt particles that are ubiquitous in coastal areas and can also be carried significant distances inland.[73] These particles are complex in composition and contain both inorganic salts and organics,[74–77] but are primarily NaCl, with smaller amounts of bromide and iodide. Schroeder and Urone[78] showed many decades ago that NO_2 at Torr concentrations reacts with NaCl to generate nitrosyl chloride (ClNO) which in the atmosphere would rapidly photolyze, generating chlorine atoms. This was extended by this laboratory to ppm concentrations,[79] supporting sea salt reactions as a potential source of atomic chlorine as an atmospheric oxidant.[80]

Atomic chlorine is even more reactive with many gas phase organic compounds than the OH radical,[81,82] which drives much of the chemistry of the atmosphere. As a result, processes which generate atomic chlorine tend to drive O_3 production through the well-known VOC-NO_x cycle.[23] Bromine atoms, on the other hand, only react with a few types of organics such as aldehydes, and hence the reaction of atomic bromine with O_3 dominates, resulting in the destruction of ozone.[83–90] Figure 17 is a schematic of the pathways that were shown in early laboratory studies to generate photochemically active chlorinated compounds that serve as chlorine atom sources in the lower atmosphere.[79,84,91–104] Of these compounds, Cl_2, $ClNO_2$, and HCl have been measured in the troposphere. It was shown that similar reactions occur for bromide in particles as well.[84,105–115] Since then, there have been a multitude of laboratory, field, and modeling studies that clearly establish the importance of halogen chemistry (including iodide) in the troposphere.[88,116–119]

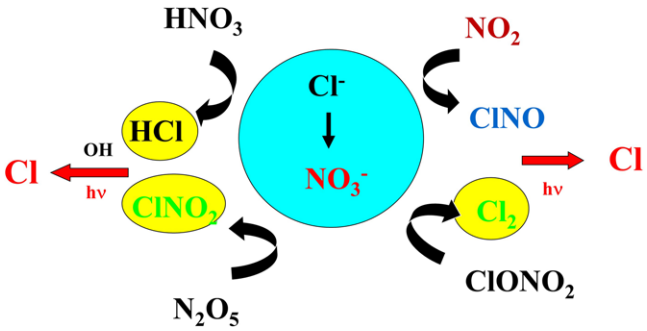

FIGURE 17 Schematic diagram of mechanisms of formation of chlorine atoms in air [Color figure can be viewed at wileyonlinelibrary.com]

Figure 18 shows the results of two studies[120,121] in which chlorine atom precursors were measured in Southern California[120] as well as in Calgary, Canada.[121] The concentrations and known photochemistry of $ClNO_2$ and Cl_2 can be used to calculate chlorine atom production rates. Measurements such as these showed that, averaged over a day at the coastal site, $ClNO_2$ photolysis was responsible for 45% of the chlorine atom production and was most important in the morning, 10% was from Cl_2 photolysis, and 45% from the reaction of HCl with OH that peaked midday.[120] In short, under some circumstances, chlorine atoms can be a significant oxidant in the troposphere, initiating the oxidation of VOC and hence the conversion of NO to NO_2 and ultimately ozone formation.

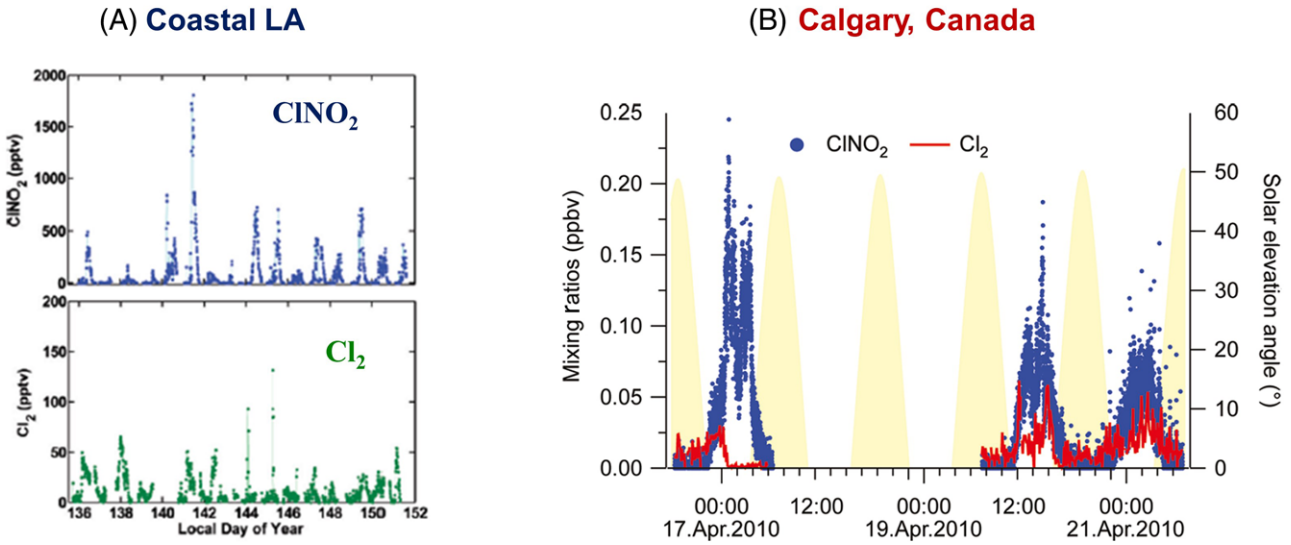

FIGURE 18 Measurements of $ClNO_2$ and Cl_2 (A) in a marine environment off the coast of Southern California[119] and (B) in Calgary, Alberta, Canada[120] [Color figure can be viewed at wileyonlinelibrary.com]

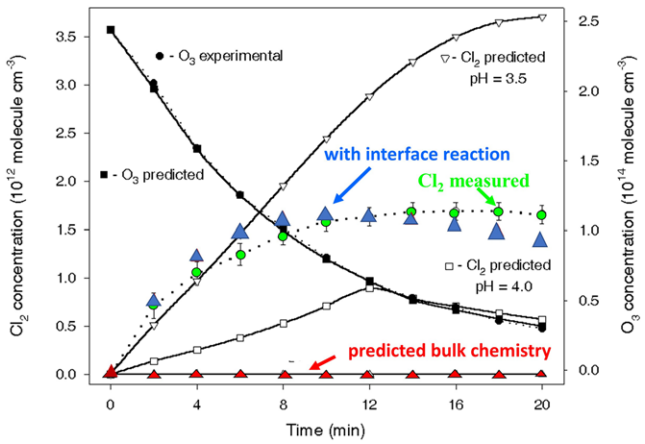

FIGURE 19 Comparison of experimentally measured Cl_2 (green circles) produced in a chamber experiment where deliquesced NaCl particles were oxidized by OH from photolysis of O_3 (black squares) in the presence of water vapor, to predictions based on known aqueous phase chemistry at several pH values with (blue triangles) and without (red triangles) the inclusion of a reaction of chloride ions at the interface with OH [Ref. 121] [Color figure can be viewed at wileyonlinelibrary.com]

An interesting aspect of halogen activation in the troposphere that arose out of combined experiment-theory studies is the presence of chloride, bromide, and iodide ions at the air-water interface of deliquesced salt particles.[84,112,122–144]

Through a combination of experiments, kinetics modeling, and molecular dynamics simulations, it was shown that the reaction of OH with Cl^- at the air-water interface was required to reconcile experimental measurements of the Cl_2 produced with the predictions from kinetics modeling.[122] One example of such a process is illustrated in Figure 19 where Cl_2 production measured in an environmental chamber (green points) is compared to that predicted using conventional processes where OH was taken up and reacted in the bulk of the particles (red triangles), with the Cl_2 generated subsequently diffusing out of the particle into the gas phase. Under this scenario, the amount of Cl_2 predicted is less than 1% of that observed. Only when a reaction of OH with Cl^- at the interface was included did the modeling results come into agreement with the experimental observations (blue triangles). Additional experiments and molecular dynamics simulations (Figure 20) showed that there is an increasing propensity of halide ions for the air-water interface as one moves down that group in the periodic table.[84,112,122–144]

In short, it is now accepted that chlorine atom generation and reactions can play a significant role in the troposphere, leading to ozone production. Bromine atoms, on the other hand, lead to ozone destruction. In any event, this is a relevant example of gas-particle reactions playing a major role in the chemistry of the lower atmosphere.

5 | HETEROGENEOUS REACTIONS OF NEONICOTINOID PESTICIDES IN THE TROPOSPHERE

The photochemistry of neonicotinoid pesticides is a final example of multiphase reactions in the atmosphere. Neonicotinoids (NNs) are systemic pesticides that came into use in the early 1990s, largely supplanting other pesticides such as the carbamates because of their lower mammalian toxicity.[145–149] They have seen increasing use, but recent evidence suggests they are at least in part responsible for negative impacts on pollinators, such as bee colony collapse.[145,150–154] As a result, three of the major NN have been banned

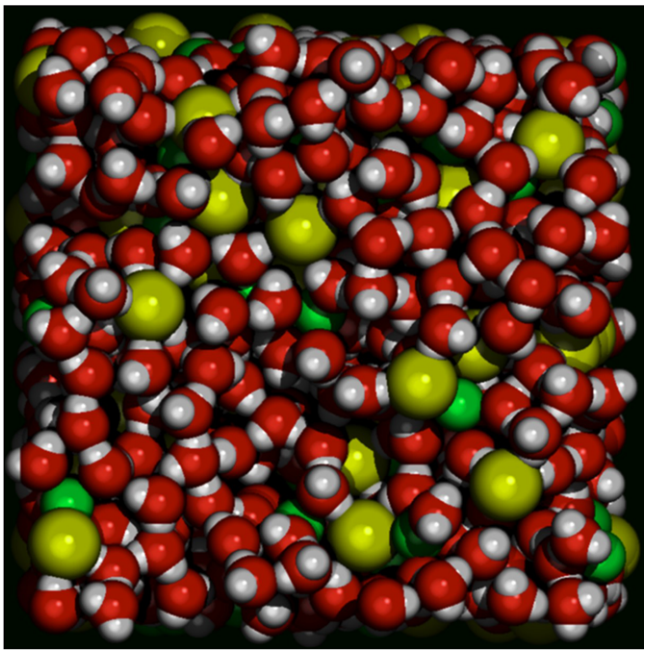

FIGURE 20 Molecular dynamics simulations of a "slab" of 96 Na^+ and 96 Cl^- with 864 water molecules. This represents a top down view, showing the chloride ions (larger yellow) being readily available to incoming gases such as OH at the interface[121] [Color figure can be viewed at wileyonlinelibrary.com]

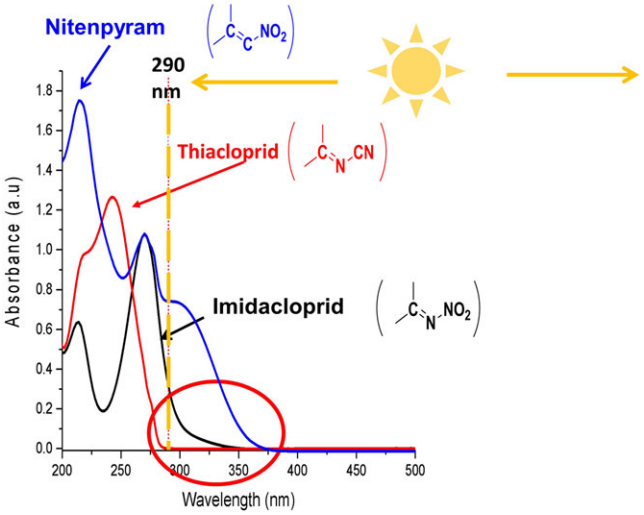

FIGURE 22 Absorption spectra of representative neonicotinoid pesticides. The actinic region at > 290 nm is indicated [Color figure can be viewed at wileyonlinelibrary.com]

for outdoor applications in the European Union[155] and in Canada.[156]

Figure 21 shows the structures of three representative neonicotinoids in use today, and the year they were introduced. Chemically, they fall into three categories: (1) nitroguanidines having a C=N−NO_2 group, (2) nitromethylenes having a C=N–NO_2 group, and (3) cyanamidines having a C = N−CN group. Figure 22 shows the UV-visible absorption spectra of one NN from each group, indicating that two of the three absorb in the actinic region, $\lambda > 290$ nm.

Imidacloprid, a nitroguanidine, has been the major NN in use, for example, as a seed coating. It is translocated throughout the plant and is subsequently taken up by sucking insects such as aphids.[146,148] Its light absorption extends out into the actinic region above 290 nm. Photolysis of a solid film of imidacloprid generates two major reaction products, a urea derivative and a desnitro derivative:[157]

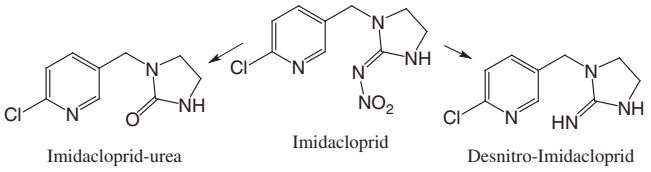

Although the desnitro product is formed in the smaller yield (16% vs 84%),[157] it has been reported to have increased mammalian toxicity compared to the parent imidacloprid.[158] This is a similar case as for the pesticide malathion, where more toxic products are formed on reaction in air.[159]

An unexpected observation was the production of N_2O as a gas phase product detected by infrared spectroscopy,[157] rather than NO_2 as might be expected from cleavage of the N−NO_2 bond in the chromophore. This was the first observation of a gas phase product from this photochemistry, and the unusual nature of the product suggested some interesting chemistry. Through the use of quantum chemical calculations, it was shown that the N−NO_2 bond should indeed undergo

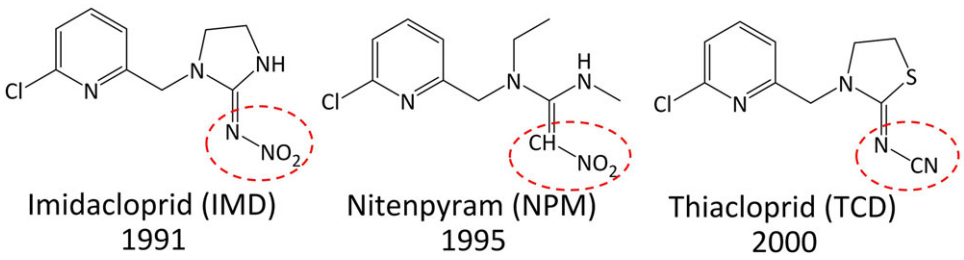

FIGURE 21 Representative examples of three types of neonicotinoids: nitroguanidines, nitromethylenes, and cyanamidines, with the years they were introduced [Color figure can be viewed at wileyonlinelibrary.com]

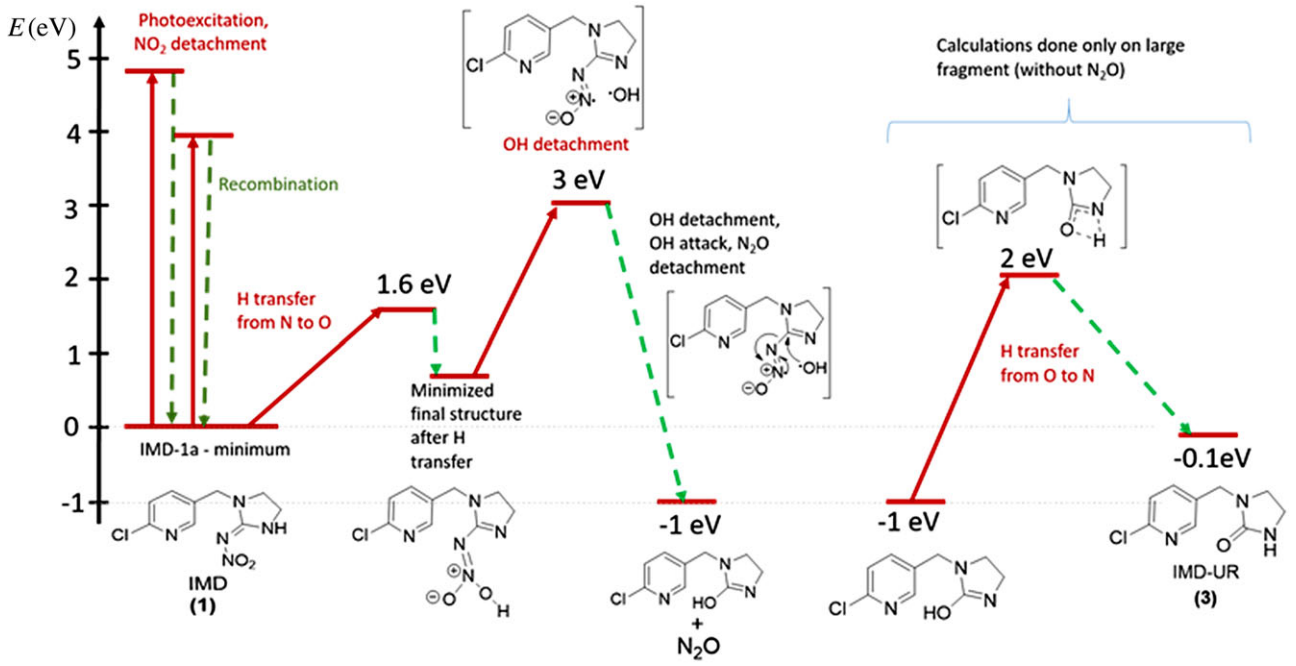

FIGURE 23 Computational studies of the photochemistry of imidacloprid showing the pathways for formation of the major solid products and gas phase N_2O [Ref. 156] [Color figure can be viewed at wileyonlinelibrary.com]

cleavage on absorption of a photon.[157] However, in the solid film, the NO_2 and nitrogen-centered radical that are generated are held in close proximity and recombine, releasing the bond energy into vibrational excitation in the ground electronic state. This excited molecule then decomposes and in a sequence of steps generates first OH and subsequently N_2O as shown in Figure 23. The generation of N_2O was shown experimentally to be characteristic of all of the nitroguanidine neonicotinoids.[160]

Quantum yields for the loss of nitroguanidine in thin solid films were recently measured to be of the order of $\sim 10^{-3}$ at wavelengths above 300 nm.[161] However, in aqueous solution the quantum yields can be one to two orders of magnitude higher.[160,162,163] This is expected, since the solvent cage is much more fluid and not as effective in holding the initially formed fragments together for the duration needed for recombination.

While the amount of nitrous oxide generated from NN photolysis on a global scale is small compared to other sources[161] and thus expected to have little impact on climate, the photolysis of the solid NN is another example of a multiphase atmospheric reaction that generates gas phase products from the condensed phase.

6 | CONCLUSIONS

In short, while the field of gas phase chemistry and photochemistry has a long and illustrious history, it is also proving to be very relevant and important in understanding multiphase chemistry in the atmosphere involving both liquids and solids. There remains much to be learned regarding the interactions of gases and particles and the detailed molecular interactions, chemistry and photochemistry that determine the impacts on health, visibility, and climate,[164] which is critical for the development of an accurate, predictive capability to address these critical issues.

ACKNOWLEDGMENTS

The author is deeply indebted to the funding agencies who have supported research in this lab over many years, particularly the National Science Foundation who have supported a wide variety of research projects. We are also grateful to the Army Research Office, the Department of Energy, and the California Air Resources Board for support. The author is particularly grateful to the many research group members who have carried out wonderful science over many years, with creativity, dedication, collaboration, and a sense of humor that has made research not only stimulating but fun. Special appreciation goes to the current research group who helped with this manuscript. Professor R. B. Gerber has been an especially patient, helpful, and creative collaborator, who with his group, is fearless about attacking new and complex problems. Without Professor Ray March's patient mentorship and introduction to the science of the atmosphere, the author would not have entered this exciting area of research. Finally, without the support and encouragement of the late Professor James N. Pitts Jr., much of this research would simply not have been carried out.

ORCID

Barbara J. Finlayson-Pitts
https://orcid.org/0000-0003-4650-168X

REFERENCES

1. Heicklen J, Westberg K, Cohen N. Report 115-69. Center for Air Environmental Studies. State College, PA: Pennsylvania State University; 1969.
2. Levy H. Normal atmosphere: large radical and formaldehyde concentrations predicted. *Science*. 1971;173:141-143.
3. Stedman DH, Morris ED, Jr, Daby EE, et al. The role of OH radicals in photochemical smog reactions. In: 160th National Meeting of the American Chemical Society, Chicago, IL; 1970.
4. Weinstock B. Carbon monoxide: residence time in the atmosphere. *Science*. 1969;166:224-225.
5. Hinds WC. *Aerosol Technology: Properties, Behavior and Measurement of Airborne Particles*. New York, NY: Wiley; 1999.
6. West JJ, Cohen A, Dentener F, et al. What we breathe impacts our health: improving understanding of the link between air pollution and health. *Environ Sci Technol*. 2016;50:4895-4904.
7. Landrigan PJ, Fuller R, Acosta NJR, et al. The Lancet commission on pollution and health. *Lancet*. 2018;391:462-512.
8. Peters A, Ruckerl R, Cyrys J. Lessons from air pollution epidemiology for studies of engineered nanomaterials. *J Occup Environ Med*. 2011;53:S8-S13.
9. Cacciottolo M, Wang X, Driscoll I, et al. Particulate air pollutants, apoe alleles and their contributions to cognitive impairment in older women and to amyloidogenesis in experimental models. *Transl Psych*. 2017;7:1-8.
10. Calderon-Garciduenas L, Solt AC, Henriquez-Roldan C, et al. Long-term air pollution exposure is associated with neuroinflammation, an altered innate immune response, disruption of the blood-brain barrier, ultrafine particulate deposition, and accumulation of amyloid beta-42 and alpha-synuclein in children and young adults. *Toxicol Pathol*. 2008;36:289-310.
11. Chen J-C, Schwartz J. Neurobehavioral effects of ambient air pollution on cognitive performance in us adults. *Neurotoxicology*. 2009;30:231-239.
12. IPCC. *Climate Change 2013: The Physical Science Basis.* Contribution of working group I to the fifth assessment report of the Intergovernmental Panel on Climate Change. Geneva, Switzerland: WMO, IPCC Secretariat; 2013.
13. IPCC. *Climate Change 2014: Synthesis Report.* Contribution of working groups I, II and III to the fifth assessment report of the Intergovernmental Panel on Climate Change. Geneva, Switzerland: WMO, IPCC Secretariat; 2014.
14. IPCC. Summary for policymakers. In: *Global Warming of 1.5°C.* An *IPCC* special report on the impacts of global warming of 1.5°*C* above pre-industrial levels and related global greenhouse gas emission pathways, in the context of strengthening the global response to the threat of climate change, sustainable development, and efforts to eradicate poverty. Geneva, Switzerland: World Meteorological Organization; 2018.
15. McNeill VF. Atmospheric aerosols: clouds, chemistry, and climate. *Annu Rev Chem Biomolec Eng*. 2017;8:427-444.
16. Samset BH. How cleaner air changes the climate. *Science*. 2018;360:148-150.
17. Ehn M, Kleist E, Junninen H, et al. Gas phase formation of extremely oxidized pinene reaction products in chamber and ambient air. *Atmos Chem Phys*. 2012;12:5113-5127.
18. Ehn M, Thornton JA, Kleist E, et al. A large source of low-volatility secondary organic aerosol. *Nature*. 2014;506:476-479.
19. Sareen N, Waxman EM, Turpin BJ, et al. Potential of aerosol liquid water to facilitate organic aerosol formation: assessing knowledge gaps about precursors and partitioning. *Environ Sci Technol*. 2017;51:3327-3335.
20. George C, Ammann M, D'Anna B, et al. Heterogeneous photochemistry in the atmosphere. *Chem Rev*. 2015;115:4218-4258.
21. Malecha KT, Nizkorodov SA. Photodegradation of secondary organic aerosol particles as a source of small, oxygenated volatile organic compounds. *Environ Sci Technol*. 2016;50:9990-9997.
22. McMurry PH. Photochemical aerosol formation from SO_2—a theoretical analysis of smog chamber data. *J Colloid Interface Sci*. 1980;78:513-527.
23. Finlayson-Pitts BJ. *Chemistry of the Upper and Lower Atmosphere—Theory, Experiments, and Applications*. San Diego, CA: Academic Press; 2000.
24. Zhao J, Smith JN, Eisele FL, et al. Observation of neutral sulfuric acid-amine containing clusters in laboratory and ambient measurements. *Atmos Chem Phys*. 2011;11:10823-10836.
25. Zollner JH, Glasoe WA, Panta B, et al. Sulfuric acid nucleation: power dependencies, variation with relative humidity, and effect of bases. *Atmos Chem Phys*. 2012;12:4399-4411.
26. Kulmala M, Kontkanen J, Junninen H, et al. Direct observations of atmospheric aerosol nucleation. *Science*. 2013;339:943-946.
27. Almeida J, Schobesberger S, Kurten A, et al. Molecular understanding of sulphuric acid-amine particle nucleation in the atmosphere. *Nature*. 2013;502:359-369.
28. Zhang RY, Khalizov A, Wang L, et al. Nucleation and growth of nanoparticles in the atmosphere. *Chem Rev*. 2012;112:1957-2011.
29. Ge XL, Wexler AS, Clegg SL. Atmospheric amines—part I. A review. *Atmos Environ*. 2011;45:524-546.
30. Ge XL, Wexler AS, Clegg SL. Atmospheric amines—part II. Thermodynamic properties and gas/particle partitioning. *Atmos Environ*. 2011;45:561-577.
31. Zhang R, Wang G, Guo S, et al. Formation of urban fine particulate matter. *Chem Rev*. 2015;115:3803-3855.
32. Phalen RF. *Inhalation Studies: Foundation and Techniques*. London, UK: Informa Healthcare; 2009.
33. Lana A, Bell TG, Simo R, et al. An updated climatology of surface dimethlysulfide concentrations and emission fluxes in the global ocean. *Global Biogeochem Cycle*. 2011;25: BG1004.
34. Whung P-Y, Saltzman ES, Spencer MJ, et al. Two-hundred year record of biogenic sulfur in a South Greenland ice core (20d). *J Geophys Res*. 1994;99:1147-1156.
35. Barnes I, Hjorth J, Mihalopoulos N. Dimethyl sulfide and dimethyl sulfoxide and their oxidation in the atmosphere. *Chem Rev*. 2006;106:940-975.
36. Karl M, Gross A, Leck C, et al. Intercomparison of dimethylsulfide oxidation mechanisms for the marine boundary layer: gaseous and particulate sulfur constituents. *J Geophys Res*. 2007;112: D15304.
37. Perraud V, Horne JR, Martinez AS, et al. The future of airborne sulfur-containing particles in the absence of fossil fuel sulfur dioxide emissions. *PNAS*. 2015;112:13514-13519.
38. Kreidenweis SM, Flagan RC, Seinfeld JH, et al. Binary nucleation of methanesulfonic-acid and water J. *Aerosol Sci*. 1989;20:585-607.

39. Wyslouzil BE, Seinfeld JH, Flagan RC, et al. Binary nucleation in acid water systems. 2. Sulfuric acid-water and a comparison with methanesulfonic acid-water. *J Chem Phys*. 1991;94:6842-6850.
40. Wyslouzil BE, Seinfeld JH, Flagan RC, et al. Binary nucleation in acid water systems. 1. Methanesulfonic acid-water. *J Chem Phys*. 1991;94:6827-6841.
41. Dawson ML, Varner ME, Perraud V, et al. Simplified mechanism for new particle formation from methanesulfonic acid, amines, and water via experiments and ab initio calculations. *PNAS*. 2012;109:18719-18724.
42. Chen H, Varner ME, Gerber RB, et al. Reactions of methanesulfonic acid with amines and ammonia as a source of new particles in air. *J Phys Chem B*. 2016;120:1526-1536.
43. Arquero KD, Xu J, Gerber RB, et al. Particle formation and growth from oxalic acid, methanesulfonic acid, trimethylamine and water: a combined experimental and theoretical study. *Phys Chem Chem Phys*. 2017;19:28286-28301.
44. Chen H, Ezell MJ, Arquero KD, et al. New particle formation and growth from methanesulfonic acid, trimethylamine and water. *Phys Chem Chem Phys*. 2015;17:13699-13709.
45. Arquero KD, Gerber RB, Finlayson-Pitts BJ. The role of oxalic acid in new particle formation from methanesulfonic acid, methylamine, and water. *Environ Sci Technol*. 2017;51:2124-2130.
46. Xu J, Finlayson-Pitts BJ, Gerber RB. Nanoparticles grown from methanesulfonic acid and methylamine: microscopic structures and formation mechanism. *Phys Chem Chem Phys*. 2017;19:31949-31957.
47. Xu J, Finlayson-Pitts BJ, Gerber RB. Proton transfer in mixed clusters of methanesulfonic acid, methylamine, and oxalic acid: implications for atmospheric particle formation. *J Phys Chem A*. 2017;121:2377-2385.
48. Xu J, Perraud V, Finlayson-Pitts BJ, et al. Uptake of water by an acid–base nanoparticle: theoretical and experimental studies of the methanesulfonic acid–methylamine system. *Phys Chem Chem Phys*. 2018;20:22249-22259.
49. Dawson ML, Xu JL, Griffin RJ, et al. Development of aroCACM/MPMPO 1.0: a model to simulate secondary organic aerosol from aromatic precursors in regional models. *Geosci Model Dev*. 2016;9:2143-2151.
50. Scovronick N, Budolfson M, Dennig F, et al. The impact of human health co-benefits on evaluations of global climate policy. *Nature Commun*. 2019;10:2095.
51. Jimenez JL, Canagaratna MR, Donahue NM, et al. Evolution of organic aerosols in the atmosphere. *Science*. 2009;326:1525-1529.
52. Noziere B, Kaberer M, Claeys M, et al. The molecular identification of organic compounds in the atmosphere: state of the art and challenges. *Chem Rev*. 2015;115:3919-3983.
53. Virtanen A, Joutsensaari J, Koop T, et al. An amorphous solid state of biogenic secondary organic aerosol particles. *Nature*. 2010;467:824-827.
54. Virtanen A, Kannosto J, Kuuluvainen H, et al. Bounce behavior of freshly nucleated biogenic secondary organic aerosol particles. *Atmos Chem Phys*. 2011;11:8759-8766.
55. Cappa CD, Wilson KR. Evolution of organic aerosol mass spectra upon heating: implications for OA phase and partitioning behavior. *Atmos Chem Phys*. 2011;11:1895-1911.
56. Perraud V, Bruns EA, Ezell MJ, et al. Nonequilibrium atmospheric secondary organic aerosol formation and growth. *PNAS*. 2012;109:2836-2841.
57. Saukko E, Lambe AT, Massoli P, et al. Humidity-dependent phase state of SOA particles from biogenic and anthropogenic precursors. *Atmos Chem Phys*. 2012;12:7517-7529.
58. Vaden TD, Imre D, Beranek J, et al. Evaporation kinetics and phase of laboratory and ambient secondary organic aerosol. *PNAS*. 2011;108:2190-2195.
59. Kidd C, Perraud V, Finlayson-Pitts BJ. New insights into secondary organic aerosol from the ozonolysis of alpha-pinene from combined infrared spectroscopy and mass spectrometry measurements. *Phys Chem Chem Phys*. 2014;16:22706-22716.
60. Kidd C, Perraud V, Wingen LM, et al. Integrating phase and composition of secondary organic aerosol from the ozonolysis of alpha-pinene. *PNAS*. 2014;111:7552-7557.
61. Hosny NA, Fitzgerald C, Vysniauskas A, et al. Direct imaging of changes in aerosol particle viscosity upon hydration and chemical aging. *Chem Sci*. 2016;7:1357-1367.
62. Reid JP, Bertram AK, Topping DO, et al. The viscosity of atmospherically relevant organic particles. *Nature Commun*. 2018;9:956.
63. Zhang Y, Sanchez MS, Douet C, et al. Changing shapes and implied viscosities of suspended submicron particles. *Atmos Chem Phys*. 2015;15:7819-7829.
64. Husar RB, Shu WR. Thermal analyses of Los Angeles smog aerosol. *J Appl Meteorol*. 1975;14:1558-1565.
65. Koop T, Bookhold J, Shiraiwa M, et al. Glass transition and phase state of organic compounds: dependency on molecular properties and implications for secondary organic aerosols in the atmosphere. *Phys Chem Chem Phys*. 2011;13:19238-19255.
66. Riipinen I, Pierce JR, Yli-Juuti T, et al. Organic condensation: a vital link connecting aerosol formation to cloud condensation nuclei (CCN) concentrations. *Atmos Chem Phys*. 2011;11:3865-3878.
67. McIntire TM, Ryder O, Gassman PL, et al. Why ozonolysis may not increase the hydrophilicity of particles. *Atmos Environ*. 2010;44:939-944.
68. Denjean C, Formenti P, Picquet-Varrault B, et al. Relating hygroscopicity and optical properties to chemical composition and structure of secondary organic aerosol particles generated from the ozonolysis of alpha-pinene. *Atmos Chem Phys*. 2015;15:3339-3358.
69. Vander Wall AC, Lakey PSJ, Rossich Molina E, et al. Understanding interactions of organic nitrates with the surface and bulk of organic films: implications for particle growth in the atmosphere. *Environ Sci Process Impacts*. 2018;20:1593-1610.
70. Domin M, Cody R. *Ambient Ionization Mass Spectrometry*. Cambridge, UK: Royal Society of Chemistry; 2015.
71. Kumbhani S, Longin T, Wingen LM, et al. New mechanism of extractive electrospray ionization mass spectrometry for heterogeneous solid particles. *Anal Chem*. 2018;90:2055-2062.
72. Wingen LM, Finlayson-Pitts BJ. Probing surfaces of atmospherically relevant organic particles by easy ambient sonic-spray ionization mass spectrometry (EASI-MS). *Chem Sci*. 2019;10:884-897.
73. Lewis ER, Schwartz SE. *Sea Salt Aerosol Production: Mechanisms, Methods, Measurements and Models. A critical REVIEW*. Washington, DC: American Geophysical Union; 2005.
74. Bertram TH, Cochran RE, Grassian VH, et al. Sea spray aerosol chemical composition: elemental and molecular mimics for laboratory studies of heterogeneous and multiphase reactions. *Chem Soc Rev*. 2018;47:2374-2400.

75. Cochran RE, Laskina O, Trueblood JV, et al. Molecular diversity of sea spray aerosol particles: impact of ocean biology on particle composition and hygroscopicity. *Chem*. 2017;2:655-667.
76. Cochran RE, Ryder OS, Grassian VH, et al. Sea spray aerosol: the chemical link between the oceans, atmosphere, and climate. *Acc Chem Res*. 2017;50:599-604.
77. Schiffer JM, Mael LE, Prather KA, et al. Sea spray aerosol: where marine biology meets atmospheric chemistry. *ACS Central Sci*. 2018;4:1617-1623.
78. Schroeder WH, Urone P. Formation of nitrosyl chloride from salt particles in air. *Environ Sci Technol*. 1974;8:756-758.
79. Finlayson-Pitts BJ. Reaction of NO_2 with NaCl and atmospheric implications of NOCl formation. *Nature*. 1983;306:676-677.
80. Finlayson-Pitts BJ. Chlorine atoms as a potential tropospheric oxidant in the marine boundary layer. *Res Chem Intermed*. 1993;19:235-249.
81. Burkholder JB, Sander SP, Abbatt JPD, et al., *Chemical Kinetics and Photochemical Data for Use in Atmospheric Studies*. Pasadena, CA: National Aeronautics and Space Administration and Jet Propulsion Lab, California Institute of Technology; 2015.
82. Ammann M, Cox RA, Crowley JN, et al. Task group on atmospheric chemical kinetic data evaluation. http://iupac.pole-ether.fr/. Accessed March 10, 2019.
83. Barrie LA, Bottenheim JW, Schnell RC, et al. Ozone destruction and photochemical reactions at polar sunrise in the lower Arctic atmosphere. *Nature*. 1988;334:138-141.
84. Foster KL, Plastridge RL, Bottenheim JW, et al. The role of Br_2 and BrCl in surface ozone destruction at polar sunrise. *Science*. 2001;291:471-474.
85. Hausmann M, Platt U. Spectroscopic measurement of bromine oxide and ozone in the high Arctic during polar sunrise experiment 1992. *J Geophys Res*. 1994;99. 25, 399-325,413.
86. Hönninger G, Platt U. The role of BrO and its vertical distribution during surface ozone depletion at Alert. *Atmos Environ*. 2002;36:2481-2489.
87. LeBras G, Platt U. A possible mechanism for combined chlorine and bromine catalyzed destruction of tropospheric ozone in the Arctic. *Geophys Res Lett*. 1995;22:599-602.
88. Simpson WR, von Glasow R, Riedel K, et al. Halogens and their role in polar boundary-layer ozone depletion. *Atmos Chem Phys*. 2007;7:4375-4418.
89. von Glasow R, von Kuhlmann R, Lawrence MG, et al. Impact of reactive bromine chemistry in the troposphere. *Atmos Chem Phys*. 2004;4:2481-2497.
90. Pratt KA, Custard KD, Shepson PB, et al. Photochemical production of molecular bromine in arctic surface snowpacks. *Nature Geosci*. 2013;6:351-356.
91. Behnke W, George C, Scheer V, et al. Production and decay of $ClNO_2$, from the reaction of gaseous N_2O_5 with NaCl solution: bulk and aerosol experiments. *J Geophys Res*. 1997;102:3795-3804.
92. Behnke W, Kruger H-U, Scheer V, et al. Formation of atomic Cl from sea spray via photolysis of nitryl chloride: determination of the sticking coefficient of N_2O_5 on NaCl aerosol. *J Aerosol Sci*. 1991;22:S609-S612.
93. Behnke W, Scheer V, Zetzsch C. Production of a photolytic precursor of atomic Cl from aerosols and Cl^- in the presence of O^3. In: Grimwall A and de Leer EWB, eds. *Naturally Produced Organohalogens*. Dordrecht, the Netherlands: Academic Publishers; 1995:375-384.
94. Behnke W, Scheer V, Zetzsch C. Formation of $ClNO_2$ and HNO_3 in the presence of N_2O_5 and wet pure nacl- and wet mixed $NaCl/Na_2SO_4$- aerosol. *J Aerosol Sci*. 1993;24:5115-5116.
95. Behnke W, Zetzsch C. Heterogeneous photochemical formation of Cl atoms from NaCl aerosol, NO_x, and ozone. *J Aerosol Sci*. 1990;21:S229-S232.
96. Zetzsch C, Behnke W. Heterogeneous photochemical sources of atomic chlorine in the troposphere. *Ber Bunsen-Ges Phys Chem*. 1992;96:488-493.
97. Zetzsch C, Pfahler G, Behnke W. Heterogeneous formation of chlorine atoms from NaCl in a photosmog system. *J Aerosol Sci*. 1988;19:1203-1206.
98. Livingston FE, Finlayson-Pitts BJ. The reaction of gaseous N_2O_5 with solid NaCl at 298 K: estimated lower limit to the reaction probability and its potential role in tropospheric and stratospheric chemistry. *Geophys Res Lett*. 1991;18:17-21.
99. Finlayson-Pitts BJ, Ezell MJ. Formation of chemically active chlorine compounds by reactions of atmospheric NaCl particles with gaseous N_2O_5 and $ClNO_2$. *Nature*. 1989;337:241-244.
100. Finlayson-Pitts BJ, Hemminger JC. The physical chemistry of airborne sea salt particles and their components. *J Phys Chem A*. 2000;104:11463-11477.
101. Gebel ME, Finlayson-Pitts BJ. Uptake and reaction of $ClONO_2$ on NaCl and synthetic sea salt. *J Phys Chem A*. 2001;105:5178-5187.
102. Hoffman RC, Gebel ME, Fox BS, et al. Knudsen cell studies of the reactions of N_2O_5 and $ClONO_2$ with NaCl: development and application of a model for estimating available surface areas and corrected uptake coefficients. *Phys Chem Chem Phys*. 2003;5:1780-1789.
103. Hoffman RC, Kaleuati M, Finlayson-Pitts BJ. Knudsen cell studies of the reaction of gaseous HNO_3 with NaCl using less than a single layer of particles at 298 K: a modified mechanism. *J Phys Chem A*. 2003;107:7818-7826.
104. Oum KW, Lakin MJ, DeHaan DO, et al. Formation of molecular chlorine from the photolysis of ozone and aqueous sea-salt particles. *Science*. 1998;279:74-77.
105. Berko HN, McCaslin PC, Finlayson-Pitts BJ. Formation of gas-phase bromine compounds by reaction of solidNaBr with gaseous $ClONO_2$, Cl_2 and BrCl at 298 K. *J Phys Chem*. 1991;95:6951-6958.
106. Finlayson-Pitts BJ, Johnson SN. The reaction of NO_2 with NaBr: possible source of BrNO in polluted marine atmospheres. *Atmos Environ*. 1988;22:1107-1112.
107. Finlayson-Pitts BJ, Livingston FE, Berko HN. Synthesis and identification by infrared spectroscopy of gaseous nitryl bromide $BrNO_2$. *J Phys Chem*. 1989;93:4397-4400.
108. Behnke W, Elend M, Kruger U, et al. The influence of NaBr/NaCl ratio on the Br^-—catalysed production of halogenated radicals. *J Atmos Chem*. 1999;34:87-99.
109. Behnke W, Scheer V, Zetzsch C. Production of $BrNO_2$, Br_2, and $ClNO_2$ from the reaction between sea-spray aerosol and N_2O_5. *J Aerosol Sci*. 1994;S25:277-278.
110. Finlayson-Pitts BJ, Livingston FE, Berko HN. Ozone destruction and bromine photochemistry at ground level in the Arctic spring. *Nature*. 1990;343:622-625.
111. Hirokawa J, Onaka K, Kajii Y, et al. Heterogeneous processes involving sodium halide particles and ozone: molecular bromine release in the marine boundary layer in the absence of nitrogen oxides. *Geophys Res Lett*. 1998;25:2449-2452.

112. Hunt SW, Roeselová M, Wang W, et al. Formation of molecular bromine from the reaction of ozone with deliquesced NaBr aerosol: evidence for interface chemistry. *J Phys Chem A*. 2004;108:11559-11572.
113. Nissenson P, Wingen LM, Hunt SW, et al. Rapid formation of molecular bromine from deliquesced NaBr aerosol in the presence of ozone and UV light. *Atmos Environ*. 2014;89:491-506.
114. Oum KW, Lakin MJ, Finlayson-Pitts BJ. Bromine activation in the troposphere by the dark reaction of O_3 with seawater ice. *Geophys Res Lett*. 1998;25:3923-3926.
115. Thomas JL, Jimenez-Aranda A, Finlayson-Pitts BJ, et al. Gas-phase molecular halogen formation from NaCl and NaBr aerosols: when are interface reactions important? *J Phys Chem A*. 2006;110:1859-1867.
116. Finlayson-Pitts BJ. The tropospheric chemistry of sea salt: a molecular-level view of the chemistry of NaCl and NaBr. *Chem Rev*. 2003;103:4801-4822.
117. Finlayson-Pitts BJ. Halogens in the troposphere. *Anal Chem*. 2010;82:770-776.
118. Saiz-Lopez A, Plane JMC, Baker AR, et al. Atmospheric chemistry of iodine. *Chem Rev*. 2012;112:1773-1804.
119. Simpson WR, Brown SS, Saiz-Lopez A, et al. Tropospheric halogen chemistry: sources, cycling, and impacts. *Chem Rev*. 2015;115:4035-4062.
120. Riedel TP, Bertram TH, Crisp TA, et al. Nitryl chloride and molecular chlorine in the coastal marine boundary layer. *Environ Sci Technol*. 2012;46:10463-10470.
121. Mielke LH, Furgeson A, Osthoff HD. Observation of $ClNO_2$ in a mid-continental urban environment. *Environ Sci Technol*. 2011;45:8889-8896.
122. Knipping EM, Lakin MJ, Foster KL, et al. Experiments and simulations of ion-enhanced interfacial chemistry on aqueous NaCl aerosols. *Science*. 2000;288:301-306.
123. Jungwirth P, Tobias DJ. Molecular structure of salt solutions: a new view of the interface with implications for heterogeneous atmospheric chemistry. *J Phys Chem B*. 2001;105:10468-10472.
124. Jungwirth P, Tobias DJ. Ions at the air/water interface. *J Phys Chem B*. 2002;106:6361-6373.
125. Liu D, Ma G, Levering LM, et al. Vibrational spectroscopy of aqueous sodium halide solutions and air-liquid interfaces: observation of increased interfacial depth. *J Phys Chem B*. 2004;108:2252-2260.
126. Gopalakrishnan S, Liu DF, Allen DC, et al. Vibrational spectroscopic studies of aqueous interfaces: salts, acids, bases and nanodrops. *Chem Rev*. 2006;106:1155-1175.
127. Jungwirth P, Tobias DJ. Specific ion effects at the air/water interface. *Chem Rev*. 2006;106:1259-1281.
128. Mucha M, Frigato T, Levering LM, et al. Unified molecular picture of the surfaces of aqueous acid, base, and salt solutions. *J Phys Chem B*. 2005;109:7617-7623.
129. Tobias DJ, Hemminger JC. Chemistry—getting specific about specific ion effects. *Science*. 2008;319:1197-1198.
130. Ghosal S, Brown MA, Bluhm H, et al. Ion partitioning at the liquid/vapor interface of a multicomponent alkali halide solution: a model for aqueous sea salt aerosols. *J Phys Chem A*. 2008;112:12378-12384.
131. Ghosal S, Hemminger JC, Bluhm H, et al. Electron spectroscopy of aqueous solution interfaces reveals surface enhancement of halides. *Science*. 2005;307:563-566.
132. Baer MD, Mundy CJ. Toward an understanding of the specific ion effect using density functional theory. *J Phys Chem Lett*. 2011;2:1088-1093.
133. Baer MD, Tobias DJ, Mundy CJ. Investigation of interfacial and bulk dissociation of HBr, HCl, and HNO_3 using density functional theory-based molecular dynamics simulations. *J Phys Chem C*. 2014;118:29412-29420.
134. Cheng MH, Callahan KM, Margarella AM, et al. Ambient pressure x-ray photoelectron spectroscopy and molecular dynamics simulation studies of liquid/vapor interfaces of aqueous NaCl RbCl and RbBr solutions. *J Phys Chem C*. 2012;116:4545-4555.
135. Gladich I, Shepson PB, Carignano MA, et al. Halide affinity for the water-air interface in aqueous solutions of mixtures of sodium salts. *J Phys Chem A*. 2011;115:5895-5899.
136. Liu JF, Zhang JZH, He X. Probing the ion-specific effects at the water/air interface and water-mediated ion pairing in sodium halide solution with ab initio molecular dynamics. *J Phys Chem B*. 2018;122:10202-10209.
137. Wick CD. A comparison of sodium and hydrogen halides at the air-water interface. *J Chem Phys*. 2017;147. https://doi.org/10.1063/1.4984114
138. Caleman C, Hub JS, van Maaren PJ, et al. Atomistic simulation of ion solvation in water explains surface preference of halides. *PNAS*. 2011;108:6838-6842.
139. Chang TM, Dang LX. Recent advances in molecular simulations of ion solvation at liquid interfaces. *Chem Rev*. 2006;106:1305-1322.
140. Frediani L, Mennucci B, Cammi R. Quantum-mechanical continuum solvation study of the polarizability of halides at the water/air interface. *J Phys Chem B*. 2004;108:13796-13806.
141. Liu DF, Ma G, Levering LM, et al. Vibrational spectroscopy of aqueous sodium halide solutions and air-liquid interfaces: observation of increased interfacial depth. *J Phys Chem B*. 2004;108:2252-2260.
142. Raymond EA, Richmond GL. Probing the molecular structure and bonding of the surface of aqueous salt solutions. *J Phys Chem B*. 2004;108:5051-5059.
143. Petersen PB, Saykally RJ. On the nature of ions at the liquid water surface. *Annu Rev Phys Chem*. 2006;57:333-364.
144. Tobias DJ, Stern AC, Baer MD. In: Johnson MA and Martinez TJ, eds. *Annu. Rev. Phys. Chem*. 2013:339-359.
145. Bonmatin JM, Giorio C, Girolami V, et al. Environmental fate and exposure; neonicotinoids and fipronil. *Environ Sci Pollut Res*. 2015;22:35-67.
146. Elbert A, Haas M, Springer B, et al. Applied aspects of neonicotinoid uses in crop protection. *Pest Manage Sci*. 2008;64:1099-1105.
147. Giorio C, Safer A, Sanchez-Bayo F, et al. An update of the worldwide integrated assessment (WIA) on systemic insecticides. Part 1: new molecules, metabolism, fate, and transport. *Environ Sci Pollut Res*. 2017:1-33. https://doi.org/10.1007/s11356-017-0394-3.
148. Simon-Delso N, Amaral-Rogers V, Belzunces LP, et al. Systemic insecticides (neonicotinoids and fipronil): trends, uses, mode of action and metabolites. *Environ Sci Pollut Res*. 2015;22:5-34.
149. Han WC, Tian Y, Shen XM. Human exposure to neonicotinoid insecticides and the evaluation of their potential toxicity: an overview. *Chemosphere*. 2018;192:59-65.
150. Botias C, David A, Horwood J, et al. Neonicotinoid residues in wildflowers, a potential route of chronic exposure for bees. *Environ Sci Technol*. 2015;49:12731-12740.

151. Raine NE, Gill RJ. Ecology: tasteless pesticides affect bees in the field. *Nature*. 2015;521:38-40.
152. Rundlof M, Andersson GKS, Bommarco R, et al. Seed coating with a neonicotinoid insecticide negatively affects wild bees. *Nature*. 2015;521:77-80.
153. van Lexmond MB, Bonmatin J-M, Goulson D, et al. Worldwide integrated assessment on systemic pesticides. *Environ Sci Pollut Res*. 2015;22:1-4.
154. Pisa L, Goulson D, Yang E-C, et al. An update of the worldwide integrated assessment (WIA) on systemic insecticides. Part 2: impacts on organisms and ecosystems. Environ. *Sci Pollut Res*. 2017. https://doi.org/10.1007/s11356-017-0341-3.
155. European Union, Document L:2018:132:TOC. *Official Journal of the European Union*, L 132, 61 May 30, 2018.
156. Pest Management Regulatory Agency, Government of Canada. Proposed re-evaluation decision PRVD2018-12, imidacloprid and its associated end-use products: pollinator re-evaluation. Ottawa, Canada; May 31, 2018.
157. Aregahegn KZ, Shemesh D, Gerber RB, et al. Photochemistry of thin solid films of the neonicotinoid imidacloprid on surfaces. *Environ Sci Technol*. 2017;51:2660-2668.
158. Chao SL, Casida JE. Interaction of imidacloprid metabolites and analogs with the nicotinic acetylcholine receptor of mouse brain in relation to toxicity. *Pest Biochem Physiol*. 1997;58:77-88.
159. Brown MA, Petreas MX, Okamoto HS, et al. Monitoring of malathion and its impurities and environmental transformation products on surfaces and in air following an aerial application. *Environ Sci Technol*. 1993;27:388-397.
160. Ezell MJ, Wang W, Shemesh D, et al. Experimental and theoretical studies of the environmental sensitivity of the absorption spectra and photochemistry of nitenpyram and analogs. Submitted.
161. Wang W, Aregahegn KZ, Andersen ST, et al. Quantum yields and N_2O formation from photolysis of solid films of neonicotinoids. *J Agric Food Chem*. 2019;67:1638-1644.
162. González-Mariño I, Rodríguez I, Roho L, et al. Photodegradation of nitenpyram under UV and solar radiation: kinetics, transformation products identification and toxicity prediction. *Sci Total Environ*. 2018;644:995-1005.
163. Todey SA, Fallon AM, Arnold WA. Neonicotinoid insecticide hydrolysis and photolysis: rates and residual toxicity. *Environ Chem Toxicol*. 2018;37:2797-2809.
164. Pöschl U, Shiraiwa M. Multiphase chemistry at the atmosphere–biosphere interface influencing climate and public health in the anthropocene. *Chem Rev*. 2015;115:4440-4475.

How to cite this article: Finlayson-Pitts BJ. Multiphase chemistry in the troposphere: It all starts… and ends… with gases. *Int J Chem Kinet*. 2019;51:736–752. https://doi.org/10.1002/kin.21305